Hindawi
Advances in Civil Engineering
Volume 2019, Article ID 3965374, 19 pages
https://doi.org/10.1155/2019/3965374

Review Article

Research Progress on Stability of Slurry Wall Trench of Underground Diaphragm Wall and Design Method of Slurry Unit Weight

Mingfeng Lei,[1,2] **Linghui Liu**,[1] **Yuexiang Lin**,[1] **Chenghua Shi**,[1] **Weichao Yang**,[1] **Chengyong Cao**,[1] **and Yao Liu**[1]

[1]*School of Civil Engineering, Central South University, Changsha, China*
[2]*Key Laboratory of Engineering Structure of Heavy Haul Railway, Central South University, Changsha, China*

Correspondence should be addressed to Weichao Yang; weic_yang@163.com

Received 22 July 2019; Accepted 19 September 2019; Published 16 December 2019

Academic Editor: Claudia Vitone

This paper performs an extensive literature survey and example investigation on the stabilisation of slurry wall trenches during the construction of diaphragm wall panel trenches, and the failure modes of slurry wall trench instability, the stability theoretical analysis models and methods, the slurry formation and its protection mechanism, the influence of related factors on slurry wall trench stabilisation, and other related problems are summarized and analyzed emphatically. And then, based on the limit equilibrium analysis method, the mechanical models of the overall stability and local stability of the trench wall are established, respectively, and the design method of slurry unit weight is derived to ensure the stability of the trench wall. Furthermore, an example application shows that the established slurry unit weight design method is reliable. At last, this paper also proposes the focus and direction for follow-up work, that is, to construct an accurate and effective theoretical analysis model of slurry wall trench instability considering the influence of multiple factors and the calculation method of the slurry cake and its mechanical or mathematical relationship with slurry quality.

1. Introduction

Diaphragm wall panel trenches are continuous underground walls with seepage proof, waterproof, and retaining and bearing functions that are formed by using digging machines to excavate narrow and deep grooves underground and pour materials inside with the help of a slurry wall [1]. Originated from Europe, the diaphragm wall panel trench excavation technology has been developed using the slurry and underwater concreting method for oil drilling [2]. Following its introduction in Milan in 1950, the slurry protection diaphragm wall panel trench was popularised in western developed countries and the former Soviet Union from the 1950s to the 1960s. This technology, which includes basic processes such as guide wall construction, slurry wall protection, trench construction, underwater concreting, and wall segment joint processing, has also become the most effective construction technology in underground and deep foundation engineering [3, 4].

The diaphragm wall panel trench excavation technology, which is characterised by small oscillations in construction processes, great wall stiffness, excellent integrity, rapid construction speed, earth rock preservation, and applicability to all geological conditions, has widely been applied in various underground projects. Japan, which owns the most advanced technology about the diaphragm wall panel trench, has constructed more than 1.5×10^7 m^2 diaphragm wall panel trench with the largest excavation depth of 140 m and lowest wall thickness of 20 cm. In 1958, the Water and Electricity Department of China built a dam cutoff wall in Danzikou Reservoir, Qingdao, using the same technology. With the rapid development of urban infrastructure in recent decades [5], the majority of the provinces of China has adopted this technology successively in constructing

diaphragm wall panel trenches as large as $1.4 \times 10^6\,m^2$ [3]. The 13th Five-Year Development Plan of China (2016–2020) proposes the construction of a $1.5 \times 10^7\,m^2$ [6, 7] diaphragm wall panel trench that will be used for new urban rail transit in the coming five years. In sum, the diaphragm wall panel trench excavation technology has great application prospects.

Despite its increasing sophistication, such technologies still have many defects, whilst its scientific norms under complex geographical conditions lack theoretical guidance. The application of this technology also frequently leads to slurry wall trench instability and failure in the actual groove construction process. Table 1 lists slurry wall trench instability accidents that typically occur in diaphragm wall panel trench construction projects around the world [8–16]. These accidents can be attributed to the defects in the quality of the wall protection slurry (i.e., uniformity and specific gravity) and the changes in the underwater level. The quality of the wall protection slurry, the mechanism of the slurry, and the influence of relative factors on slurry wall trench stability during the construction of a diaphragm wall panel trench must be understood as they directly affect the safety of the project. Therefore, this paper examines the issues related to the stability of these trenches by performing an extensive literature review and emphasizes the diaphragm wall panel trench instability failure modes, the computation method, the slurry wall protection mechanism, and the relative factors that affect slurry wall trench stability to provide a valuable reference for follow-up studies and engineering applications.

2. Diaphragm Wall Panel Trench Instability Modes

Many scholars believe that the diaphragm wall panel trench instability modes can be divided into overall instability and local instability (Figure 1). The slurry wall trench instability for soft ground with a certain bonding property is reflected in the global sliding, whilst that for a weak interlayer with weak or without bonding property is mainly reflected in the local instability of the spot scale off.

2.1. Overall Instability. Accident investigations, models indoor, and field tests show that the overall instability of the slurry wall trench often occurs 5 m to 15 m deep in surface or shallow soil [10, 12, 17–19]. A bulge can also be found in the soil under the guide wall [19]. The instability failure surface is spread along the whole length of the groove on the ground surface and takes the shape of an oval or rectangle [13, 16], as shown in Figure 1(a). Moreover, the slurry wall trench can easily become unstable when the slurry level is reduced to 1 m below the water level or when the ground is overloaded [10]. Also, minor structure planes (thin weak interlayers or shear bands) may affect the overall stability behaviour of geological systems in varying degrees [20].

2.2. Local Instability. When the foundation soil has a weak interlayer and poor bonding property (such as sand-cobble stratum) and when the seepage force of the slurry cannot maintain its balance with the pressure of the slurry wall trench soil, the slurry wall trench also experiences the local instability and often shows an overexcavation of pit [21], as indicated in Figure 1(b). Consequently, the filling coefficient of the concreting or impervious material increases, thereby increasing the construction cost and difficulty [22, 23].

3. Analysis of Diaphragm Wall Panel Trench Stability

Many scholars have examined slurry wall trench stability since the introduction of the diaphragm wall panel trench technology [13, 24]. Along with the wide application of this technology, related studies have produced rich results from their field or laboratory tests [12, 25], numerical simulations (e.g., elasto-plastic FEM with the shear strength reduction technique [26], anisotropic visco-hypoplastic FEM [27], and upper and lower bound limit FEM [28]), and theoretical analyses, amongst which the theoretical analyses have produced the most outputs and resulted in the introduction of 10 additional computation models or analysis methods. Table 2 and Figure 2 present the theoretical analysis models and methods for slurry wall trench stability with many reference applications [1, 10, 18, 19, 21, 25, 29–43]. These models can be divided into two categories, namely, 2D and 3D analysis methods, by considering the soil arching effect on the water level, as shown in Figure 3. The 2D methods can be divided into the analysis method for the stress limit state of the element soil, the analysis method for soil pressure balance on both sides of the slurry wall trench, and the analysis method for the force balance of the plane sliding body according to the mechanical principle, as shown in Table 2 and Figure 3. Figure 4 presents the definitions of all parameters.

3.1. Analysis Method for the Stress Limit State of the Element Soil. This method uses the relative ratio $F_s = r_3/r_2$ to evaluate the stability of the slurry wall trench, where F_s is the safety factor, r_2 is the radius of the effective stress Mohr's circle of the element soil on the slurry wall trench after excavation, r_3 is Mohr's circle tangent radius of the shear strength enveloping line with pore water pressure dissipation, as shown in Figure 5. Jiang et al. [29] used this method to explore the time effect problem of slurry wall trench stability and the influence of the changes in pore water pressure on the stability of the slurry wall trench during slot excavation. The negative pore water pressure from the excavation unloading of slot soil was conducive to slurry wall trench stability. The negative pore water pressure gradually dissipated to reduce the long-term stability of the slurry wall trench. Liu et al. confirmed the usefulness of this method in exploring the effect of overload on slurry wall trench stability [30].

3.2. Analysis Method for the Soil Pressure Balance on Both Sides of the Slurry Wall Trench. This method evaluates the stability of the slurry wall trench by comparing the valid

Table 1: Incidents of groove wall collapse in diaphragm wall panel trench construction projects.

Year	Projects	Project profile				Destruction	
		Formation condition	Groundwater level (m)	Diaphragm trench parameters (depth × thickness) (m)	Slurry volume/ weight (kN/m^3)	Destructive body	Causes
1983	Rhine river bank, Germany	Sandy soil	−1.5	(26–30) × (3–5)		Collapse surface expanded from the ground surface to 12 m deep into the groove wall	Soft formation without a bonding property
1982	Hong Kong, China	Back fill, marine fine sand, sludge, and sedimentary soil	−3.0	35 × 1	10.58	Collapse surface expanded from 4 m behind the wall to 7 m deep into the wall	Drop in the slurry level
1984	Hong Kong, China	Back fill, marine deposit, and strongly weathered granite		2.7 m long excavated group	10.5	The groove wall collapsed and expanded 5 m–12 m deep into the ground surface	Drop in the slurry level
2013	Suzhou railway station, China	Powder soil and sandy soil	High groundwater level with pressure-bearing water	58.6 × 1.8		A collapse occurred in two groove segments at the beginning. For the first segment, the groove wall collapsed as the reinforcement cage was placed into the groove, thereby scrapping the reinforcement cage. For the second segment, a great collapse suddenly occurred in the groove wall during the clearance process, thereby burying the trench grab	The formation is soft and has a poor self-stabilising ability
2000	Eastern part of Tainan, Chinese Taipei	Powder sand	−3.0	15 × 0.9	10.5	The diaphragm wall panel trench was destroyed. and cracks appeared 4.5 m behind the wall, thereby leading to a hemispherical soil collapse	Drop in the slurry level

Table 1: Continued.

Year	Projects	Project profile				Destruction	
		Formation condition	Groundwater level (m)	Diaphragm trench parameters (depth × thickness) (m)	Slurry volume/ weight (kN/m^3)	Destructive body	Causes
1994	Near a river bank in France	Alluvial soil containing many eggs		—	17.6–18.6	The length and width of the collapse were the same. The depth was located at the bottom of the back fill. The destructive shape was of the Kulun wedge type	Flash flood and an increase in the groundwater level
2003	Osaka, Japan	Back fill	−2.2	(20–40) × 0.8	11.3	The surfaces of the diaphragm wall were in contact with each other, thereby leading to collapse	The formation cannot self-stabilise
1998	Southwest coast of Chinese Taipei	Back fill and weak layer of marine clay soil from 10 m to 11.5 m	−3.0	(20–40) × 0.8		The diaphragm wall was destroyed at the layer of the marine clay soil	A single excavation takes up much time
2002	Hebei Huangbizhuang reservoir, China	Loam, medium sand, coarse sand at the lower part, fine sand in the local part, pebble bed, and crushed stone layer		—		The collapse mainly occurred 5 m–9 m deep into the wall, whereas the plane showed an oval shape and spread along the direction of the pore	Loss in slurry burst
1999	Huangsha line, line 1, Guangzhou subway 1, China	Sandy soil	−6.5	17 × 0.6	10.6	The wall collapsed from the surface down to 6 m, whilst the plane expanded to 4 m outside the pit	Low slurry indexes and high pore water pressure
2010	Cutoff wall for the main dam and the first and second auxiliary dams of Ying river bank, China	Clay sand	−3.0	(>30) × 0.6	10.3	The groove wall entirely collapsed after a hydraulic grab was used to excavate 10 m and 30 m deep into the wall	The slurry was unevenly stirred, and the hydraulic grab rapidly went up and down, thereby leading to a rapid erosion

slurry pressures on both sides of the slurry wall trench ($p_s - p_w$) with the soil pressure considering that the soil is influenced by vertical surface p, that is, $F_s = (p_s - p_w)/p$. This method focuses on how soil pressure p can be calculated and confirmed considering the soil arc effect in the vertical surface. Schneebeli [10, 31] and Huder [32] investigated this problem and proposed novel methods for calculating the horizontal soil pressure p on the slurry wall trench element soil based on Caquot's and Terzaghi's soil arc theory, as shown in equations (1) and (2). Wong [10] and Hajnal et al. [31] proposed a method

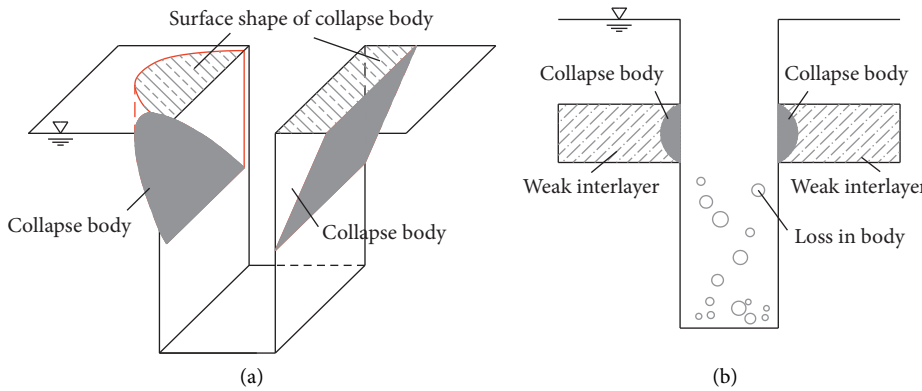

Figure 1: Instability modes of trench wall: (a) overall instability; (b) local instability.

Table 2: Statistics of theoretical analysis models or methods on trench wall stability.

Literature resources	Models	Computational formulas
Jiang et al. [29], Liu et al. [30]	—	$F_s = [\gamma h_w + (\gamma' - \gamma_w)(d - h_w) + \gamma_s(d - h_s) + q]\sin\varphi' + 2c'\cos\varphi' / [\gamma h_w + (\gamma' + \gamma_w)(d - h_w) - \gamma_s(d - h_s) + q]$
Schneebeli [10, 31], Wong [10], Huder [32], Hajnal et al. [31]	—	When $z \le h_w$, $p = K_a[(\gamma l/\sin 2\varphi')(1 - e^{(-z/l)\sin 2\varphi'}) + qe^{(-z/l)\sin 2\varphi'}] - 2c'\tan(45^\circ - (\varphi'/2))$, $K_a = (1 - \sin\varphi')/(1 + \sin\varphi')$
	—	When $z > h_w$, $p = K_a[(\gamma l/\sin 2\varphi') + ((\gamma - \gamma')l/\sin 2\varphi')e^{((h_w - z)/l)\sin 2\varphi'} - (\gamma l/\sin 2\varphi')e^{(-z/l)\sin 2\varphi'} + qe^{(-z/l)\sin 2\varphi'}] - 2c'\tan(45^\circ - \varphi'/2)$
	—	When $z \le h_w$, $p = ((\gamma l - 2c')/2\tan\varphi')(1 - e^{-2(z/l)K\tan\varphi'}) + Kqe^{-2(z/l)K\tan\varphi'}$
	—	When $z \le h_w$, $p = ((\gamma' l - 2c')/2\tan\varphi') + ((\gamma - \gamma')l/2\tan\varphi')e^{-2((z - h_w)/l)K\tan\varphi'} - ((\gamma l - 2c')/2\tan\varphi')e^{-2(z/l)K\tan\varphi'} + Kqe^{-2(z/l)K\tan\varphi'}$
Morgenstern and Amir-Tahmasseb [13]	Figure 2(a)	$\gamma_s' = (d/(d - h_s))^2[(1 - \sin\varphi')/(1 + \sin\varphi')\gamma + ((d - h_w)/d)(2\sin\varphi'/(1 + \sin\varphi'))\gamma_w]$
Washbourne [19]	Figure 2(c)	$P = (l^2/4)[(\gamma - \gamma')h_w + \gamma'(d - (l/6))]\tan^2(45^\circ - (\varphi'/2)) - (c'l^2/2)\tan(45^\circ - (\varphi'/2))$
Yang et al. [33–35], Li [36]	Figure 2(d)	$P = (l\tan(\alpha - \varphi')/8)\{\gamma' l(\pi d - (2/3)l\tan\alpha) + \pi l\gamma_w h_w + \pi l q - 4c'(\pi d - l\tan\alpha) - \pi c' l[\tan\alpha + 1/\tan(\alpha - \varphi')]\}$
Ji and Yu [37]	Figure 2(f)	$P_s - P_w = (\gamma_s l/3d)(d^2 - h_s^2)^{3/2} - (\gamma_w l/3d)(d^2 - h_w^2)^{3/2}$; $\beta = \arcsin(h_w/d)$; $\theta = \arcsin(l/2d)$, $P = (l^2\cot(\theta + \varphi')/48\cos\theta)\{3\pi\gamma h + 6\pi q - 24c'[\cot\theta + (1/\cot(\theta + \varphi'))] + (\pi - \sin 2\beta - 2\beta) \times (3\gamma h_w + 2\gamma' d - 2\gamma' h_w)\}$
Piaskowski and Kowalewski [38], Zhang and Xia [39]	Figure 2(g)	$\gamma_s = (K_A/(h_m - h_s))[\sum_{i=1}^{k}\Delta h_i\gamma + \sum_{i=k+1}^{k}\Delta h_i\gamma'] + [\gamma_w(h_m - h_w)/(h_m - h_s)]$ $P = 2w_f l[\gamma_w h_w + q + (\gamma - \gamma_w)(d - (2/5)w_f\tan\varphi')](\sin\alpha - \cos\alpha\tan\varphi')/3(\cos\alpha + \sin\alpha\tan\varphi') - w_f c'((2l/\cos\alpha) + 6d - 3w_f\tan\alpha)/3(\cos\alpha + \sin\alpha\tan\varphi')$

for calculating soil pressure p considering the overloading based on the above theories:

$$\sigma_3 = \frac{\gamma L}{\sin(2\phi)}\tan^2\left(\frac{\pi}{4} - \frac{\phi}{2}\right)\left(1 - \frac{z}{L}e^{-\sin(2\phi)}\right), \quad (1)$$

$$\sigma_3 = \frac{\gamma L}{2\tan\phi}\left(1 - \frac{z}{L}e^{-2K\tan\phi}\right), \quad K_0 > K > K_a, \quad (2)$$

where σ_3 is the horizontal stress of the soil on the pore wall, as shown in Figure 5, L is the length of the slot pore, γ is the density of soil on the slurry wall trench, ϕ is the internal friction angle of soil on the slurry wall trench, and K is the earth pressure coefficient of the soil arc effect. The value of K is within the range of the active and static earth pressure coefficients K_a and K_0.

3.3. Analysis Method for the Force Balance of the Plane Sliding Body. This method is divided into the limit equilibrium method of the rigid sliding block and the limit analysis method based on upper bound theory considering the internal energy dissipation of the sliding block. Both of these methods use the ratio $F_s = \tau_f/\tau$ to evaluate the stability of the slurry wall trench according to the assumed sliding

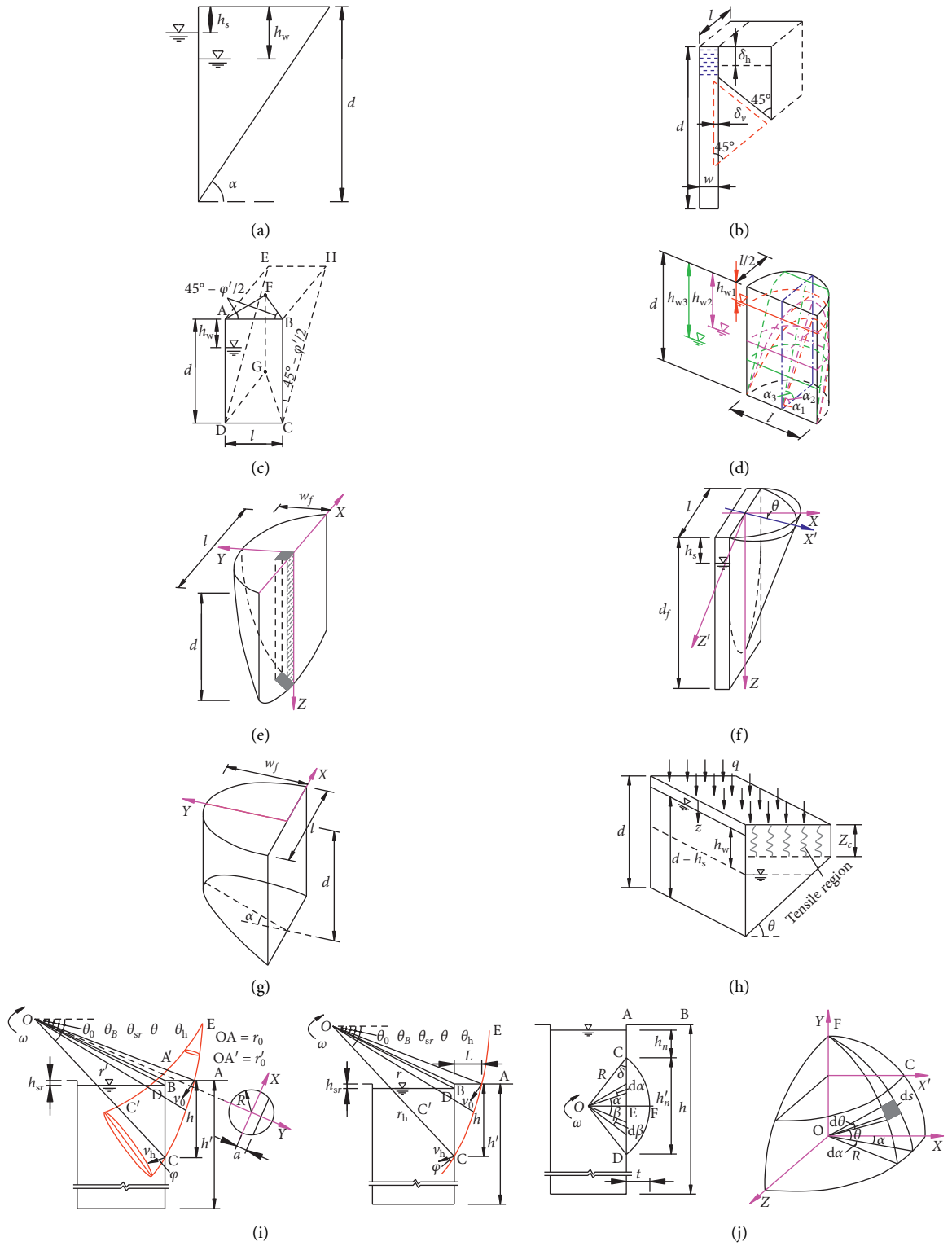

Figure 2: Typical theoretical analysis models of trench wall: (a) Bevel mode [13, 25]; (b) Bevel and vertical plane mode [18]; (c) triprism mode [19]; (d) half-cylinder modes [33–36]; (e) shell-type mode [40]; (f) half-cylinder with the oblique section mode [37]; (g) parabolic mode [38, 39]; (h) Coulomb slide mass mode [41]; (i) 3D and 2D limit analysis model for overall instability [42]; (j) 2D and 3D limit analysis model for local instability [21].

surface, where τ_f is the shear strength of soil and τ represents the required shear strength for the equilibrium slide on the boundary sliding surface of slide. Morgenstern and Amir-Tahmasseb [13] established a slurry wall trench stability analysis model, as shown in Figure 2(a), based on different assumed broken faces, and explored the influence

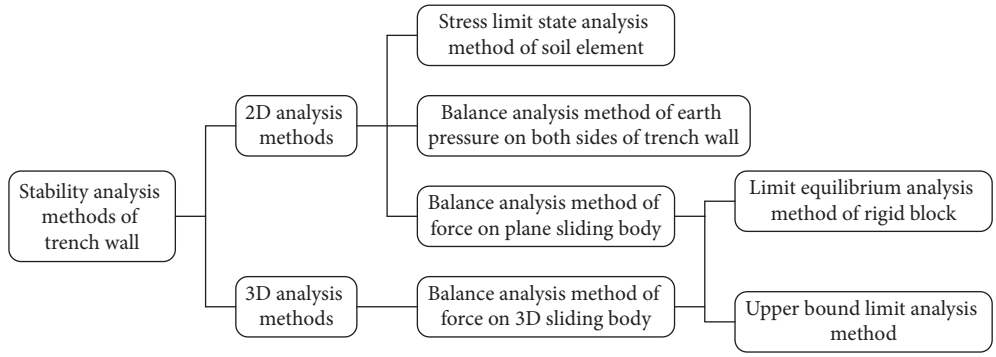

Figure 3: Analysis methods classifications of trench wall stability.

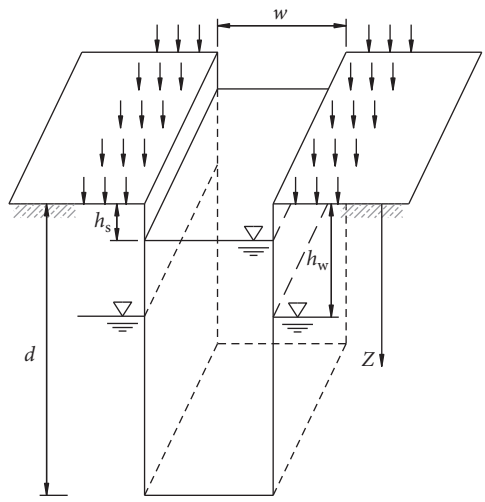

γ_s: volume-weight of slurry
γ: volume-weight of soil
γ': effective volume-weight of soil
φ: internal friction angle of soil
c: cohesion of soil

Figure 4: Schematic diagram of diaphragm wall panel trench.

of different factors on slurry wall trench stability based on this model. In sum, the accuracy of the results calculated by this method directly depends on the assumption of the sliding surface. Such assumptions may differ across various soil types, overloading conditions, and other factors. Therefore, a reasonable sliding surface must be set in practical applications.

3.4. Force Balance Analysis Method. Force balance analysis method of the 3D sliding body is also divided into two methods, namely, the limit equilibrium method and the limit analysis method based on upper bound theory. Both of these methods consider the influence of the soil arc effect on the horizontal of the foundation soil surrounding the slurry wall trench. According to the assumed 3D sliding body, the effective slurry pressure that acts upon the slurry wall trench is compared with the pressure for the equilibrium sliding body $F_s = (P_s - P_w)/P$, whilst the soil shear strength is compared with the shear force used for the self-weighing of the equilibrium sliding body on the boundary sliding surface of sliding body $F_s = \tau_f/\tau$ to evaluate slurry wall trench stability. Nearly 10 analysis models have been successively proposed in the literature [18, 19, 21, 33–37, 39, 40, 42, 43], as shown in Figure 2.

The above analysis reveals that various models have different mechanical principles, methods, and factors. In this case, the adaptability and reliability of their calculation results greatly differ. Wang et al. [44] performed a comparative analysis and found that the 2D analysis method was too conservative or generated unstable calculation results. Relatively speaking, the semiterete and triprism sliding model can reasonably evaluate slurry wall trench stability in sandy formation; if the relationship between the sliding body and the groove depth on the plane is established using the 3D analysis methods, then the calculation result becomes very conservative. Therefore, this study focuses on the establishment of a reasonable and effective slurry wall trench stability theory model and method.

4. Formation and Wall Protection Mechanism of Slurry

4.1. Formation Mechanism of Slurry. The slurry must have a certain film-forming property, physical and chemical stability, liquidity, and proper density. The slurry includes bentonite slurry, polymer slurry, CMC slurry, and saline solution slurry [45], amongst which the bentonite slurry is the most widely applied because of its excellent function and economic value [46].

The bentonite slurry mainly comprises bentonite, water, and admixture. Bentonite is a granular clay soil with great viscosity and plasticity that will greatly expand if submerged in water. This material has a thixotropic property, wet expansion performance, colloid properties, and montmorillonite as its main component. As shown in Figure 6, montmorillonite follows a Si–Al–Si three-layer structure and has an amorphous plate surface that can easily absorb positive ions. After mixing bentonite with clean water, the water rapidly enters into grid work of the montmorillonite, results in significant swelling, and

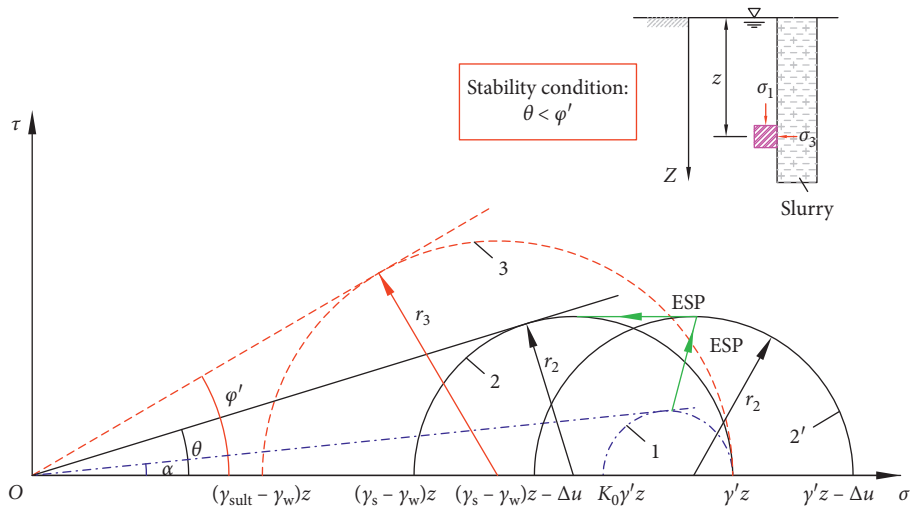

γ_s: volume-weight of slurry
γ': effective volume-weight of soil
γ_w: volume-weight of water
γ_{sult}: ultimate volume-weight of slurry
Δu: negative pore water pressure
K_0: effective coefficient of earth pressure at rest

1: initial state
2′: state after excavation with Δu
2: state after excavation without Δu
3: ultimate state
EPS: stress paths

Figure 5: Mechanical principle of stress limit state analysis method of soil element [29].

becomes a negatively charged hydrophilic colloid to disperse and suspend bentonite particles and to form a slurry, as shown in Figure 7.

4.2. Mechanics of Slurry Wall Protection. The slurry wall protection can be divided into two types based on its mechanics, namely, the hydrostatic pressure action and the gelling effect of the slurry [47], as shown in Figure 8.

4.2.1. Hydrostatic Pressure Action. Under a specific gravity, the slurry produces some hydrostatic pressure P_s on the wall. This pressure can resist the lateral active earth and water pressures $(P_a + P_w)$ that act upon the slurry wall trench. Acting as liquid support, the slurry can prevent the collapse and peeling of the slurry wall trench as well as the infiltration of groundwater. By neglecting the negative pore water pressure during groove excavation, the following expression is used:

$$\begin{cases} P_s = \dfrac{\gamma_s z^2}{2}, \\ P_a + P_w = \dfrac{(K_a\gamma' + \gamma_w)z^2}{2}, \end{cases} \tag{3}$$

Based on the above expression, we can judge the slurry wall trench stability after excavation according to the actual density of the slurry or calculate the designed density of the slurry according to the required stability of the slurry wall trench as follows:

$$\begin{aligned} F_s &= \frac{P_s}{P_a + P_w}, \\ &\text{or } \frac{\gamma_s}{K_a\gamma' + \gamma_w}, \\ \gamma_s &= [F_s](K_a\gamma' + \gamma_w), \end{aligned} \tag{4}$$

where $[F_s]$ refers to the designed safety factor.

The above analysis reveals that the essence of mud hydrostatic pressure can be regarded as the stress state of the soil in the slurry wall trench. To guarantee slurry wall trench stability, the radius of Mohr's circle of stress of the soil in the slurry wall trench r_2 after excavation under slurry pressure must be less than the radius of Mohr's circle of stress r_3 at its limited state. In other words, Mohr's circle of stress 2 of the soil in the slurry wall trench after excavation must range between Mohr's circle of stress at the beginning 1 and the limited Mohr's circle of stress 3, as shown in Figure 5.

4.2.2. Gelling Action of the Slurry. On the one hand, the slurry will form a layer of mud cake with very low water permeability on the slurry wall trench during the penetration of mud into the soil [48], as shown in Figure 8. The hydrostatic pressure of the slurry can effectively act on the slurry wall trench to prevent the spalling of soil particles. On the other hand, the slurry will penetrate from the surface of the slurry wall trench into the soil. Upon penetrating to a certain range, the slurry will adhere to the soil particles to resist the soil particles in the hole that are peeled from the slurry wall trench, thereby increasing the stability of the slurry wall trench. Gill [49] showed that when the slurry

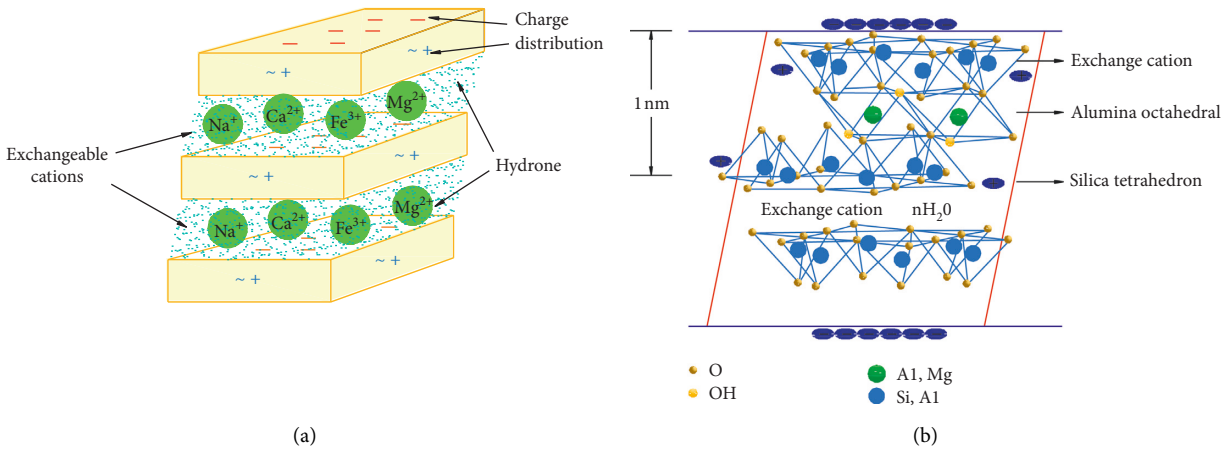

Figure 6: Chemical construction of montmorillonite.

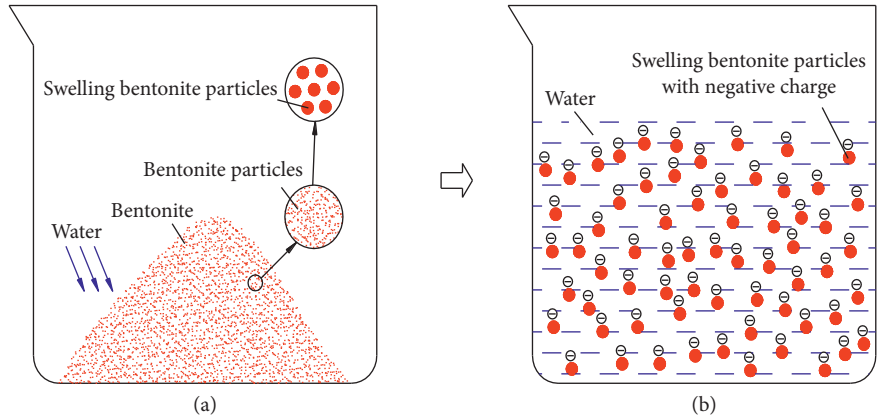

Figure 7: Forming process of bentonite slurry.

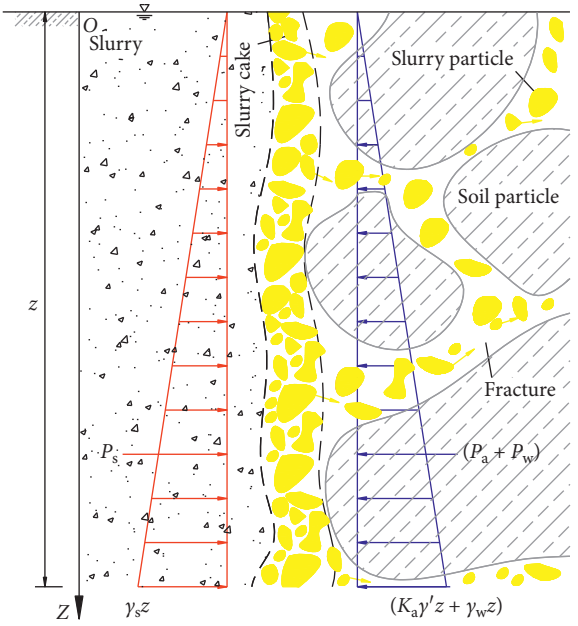

Figure 8: Wall protection mechanism of slurry [47].

pressure is 65% to 80% of the active earth pressure, the slurry wall trench is generally unstable. The stability of the slurry wall trench mainly depends on the gelling action of the slurry. Figure 9 analyses the gel microunit of the slurry. The equilibrium equation of the slurry microunit can be obtained as follows:

$$\begin{aligned} \frac{\partial \sigma_x}{\partial x} + \frac{\partial \tau_{xz}}{\partial z} &= 0, \\ \frac{\partial \sigma_z}{\partial z} + \frac{\partial \tau_{xz}}{\partial x} - \gamma_s &= 0. \end{aligned} \tag{5}$$

The slurry achieves plastic flow when the stress state of the microunit satisfies the yield condition $(\sigma_x - \sigma_z)^2 + 4\tau_{xz} = 4\tau_s^2$, where τ_s is the shear strength of the slurry gel. Under appropriate conditions, equation (5) can be used to obtain the static stress of the groove hole. For the groove hole with a width of $w = 2b$, the Bishop solution can be used to obtain its horizontal stress as follows:

$$\sigma_x = \gamma_s + \left(\frac{\pi}{2} + \frac{z}{b}\right)\tau_s. \tag{6}$$

The horizontal total resistance generated from the slurry gel is computed as follows:

$$P_s = \int_0^z \sigma_x \mathrm{d}z = \frac{1}{2}\gamma_s z^2 + \frac{1}{2b}\tau_s z^2 + \frac{\pi}{2}\tau_s z. \tag{7}$$

Based on the above formula, the horizontal stress produced in the soil increases along with the shear strength of the slurry gel and the stability of the groove hole. Therefore, high-quality slurry must be used in practice. The slurry consistency increases to gain a certain shear strength, whilst the gelling action increases to improve the stability of the slurry wall trench.

5. Design Method of Slurry Unit Weight Based on Groove Wall Stability

Based on the above research status analysis, in this section, an analysis model is established from the aspects of overall stability and local stability of the slurry trench wall, and the critical slurry weight design method is derived based on the limit equilibrium method, so as to provide theoretical basis for engineering practice.

5.1. Calculating Method for Slurry Unit Weight considering Overall Stability of Trench Wall. The cavity formed after trench excavation of underground diaphragm wall is similar to that of foundation pit. Therefore, the mechanical analysis model of overall stability of trench wall can be established by referring to the surrounding stratum stability analysis model after excavation of foundation pit and assuming that the soil mass within the depth of the trench is a single homogeneous body, as shown in Figure 10.

Take the cross section shown in Figure 10 for force analysis and set up its analysis diagram according to the actual force on the trench wall, as shown in Figure 11. Then, according to the balance of the force, the stability coefficient F_s of the sliding body is

$$F_s = \frac{(\Delta P - P_a)\cos\alpha + T_1 + T}{(W + Q)\sin\alpha}, \tag{8}$$

where F_s is the stability coefficient of trench wall, taking 1.2~1.5; Q is the resultant force of ground overload; W is the dead weight of the sliding body; P_s is the resultant pressure of slurry; P_w is the combined pressure of groundwater; P_a is the active earth pressure resultant force on the sliding body; H_s is the distance from the slurry surface to the ground; T_1 and N are, respectively, the tangential force and normal force on the OCDE of the inclined plane at the bottom of the sliding body; and T_2 is the cohesive force of soil mass on ACOF (BDEG) vertical planes on both sides of the sliding body. Calculate as follows:

$$\begin{cases} W = \dfrac{L^2\cos\alpha}{2\tan\varphi}\left[\gamma H_w + \gamma'\left(H - H_w - \dfrac{L\sin\alpha}{4\tan\varphi}\right)\right], \\ \Delta P = \dfrac{1}{2}L\left[\gamma_s(H - H_s)^2 - \gamma_w(H - H_w)^2\right], \\ Q = qL^2\dfrac{\cos\alpha}{2\tan\varphi}, \\ P_a = L\displaystyle\int_0^{H_w}\left[K_a(\gamma h + q) - 2c\sqrt{K_a}\right]\mathrm{d}h \\ \qquad + L\displaystyle\int_{H_w}^{H-H_{cr}}\left[K_a\left(\gamma H_w + \gamma'(h - H_w) + q\right) - 2c\sqrt{K_a}\right]\mathrm{d}h, \\ T_1 = N\tan\varphi + cS_{\square OCDE}, \\ T_2 = c\left(S_{\square ACOF} + S_{\square BDEG}\right), \end{cases} \tag{9}$$

where γ is the average weight of soil above the surface of groundwater, γ' is the floating weight of soil below the groundwater plane, ΔP is the combined force of slurry pressure on trench wall and groundwater pressure, γ_s is the mud weight, K_a is the active earth pressure coefficient, $N = (W + Q)\cos\alpha + (\Delta P - P_a) \times \sin\alpha$, $S_{\square OCDE}$ is the area of the sliding surface, c is the average cohesive force of soil mass, and $S_{\square ACOG}$ and $S_{\square BDEF}$ are the areas of ACOF and BDEG on the vertical side, respectively.

5.2. Calculating Method for Slurry Unit Weight considering Local Stability of Trench Wall. It is assumed that the local sliding body on the unilateral groove wall is a semicylinder with radius a, as shown in Figure 12, and then the local stability analysis model, as shown in Figure 13, can be established. As shown in Figure 13, the force analysis of the upper and lower microsoil strip elements is conducted by taking the upper and lower microsoil strip elements, respectively, and the force diagram of

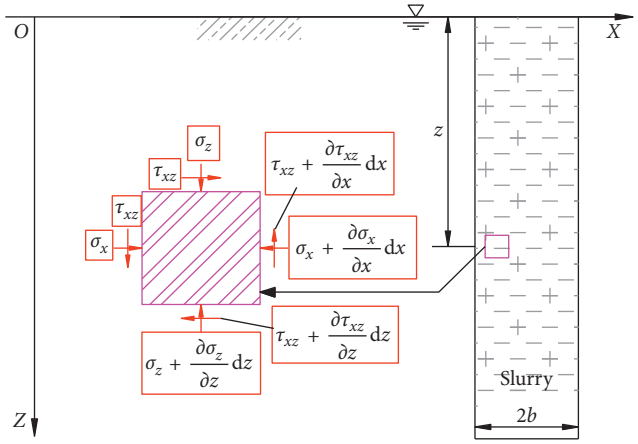

Figure 9: Force analysis diagram of gel slurry.

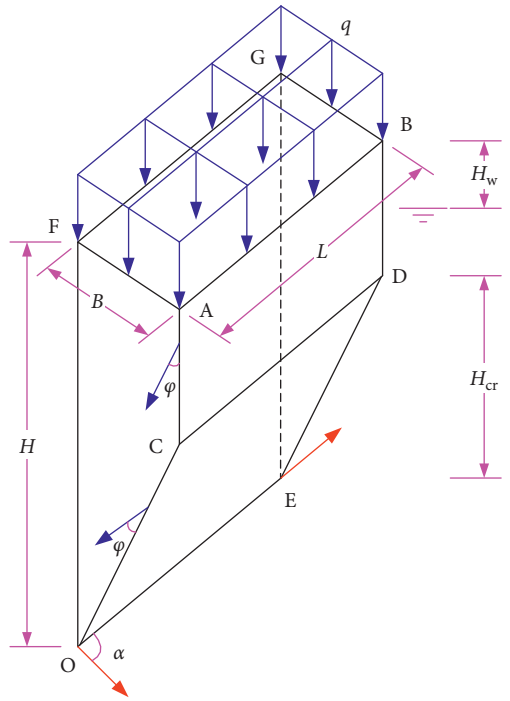

Figure 10: Mechanical model for overall stability analysis of slot wall. φ is the effective internal friction angle of soil mass; α is the angle between the OEDC and the horizontal plane, $\alpha = 45^\circ + (\varphi/2)$; L is the length of trench section; B is the width of sliding body, $B = H_{cr} \cot \alpha$, where $H_{cr} = L \sin \alpha / 2 \tan \varphi$; q is the ground overload; H is the depth of sliding body; H_w is the buried deep for the water table.

each soil strip can be obtained by ignoring the horizontal interaction between the soil strips. From the static equilibrium conditions $M = 0$ of the local sliding body relative to point O, the following equation can be obtained:

$$M_1 + M_2 = M_3 + M_4, \tag{10}$$

where M_1 and M_2 are, respectively, the sliding moments of local sliding body relative to point O caused by water pressure and dead weight and M_3 and M_4 the antislip moment of local sliding body caused by mud pressure and shear force relative to point O. Specifically, it can be calculated as follows:

$$\begin{cases} M_1 = \dfrac{2\gamma' a^3}{3}, \\ M_2 = \dfrac{2\gamma_w a^3}{3}, \\ M_3 = \dfrac{2\gamma_s a^3}{3}, \\ M_4 = \displaystyle\sum_{i=1}^{n} T_i a + \sum_{j=1}^{n} T_j a, \end{cases} \tag{11}$$

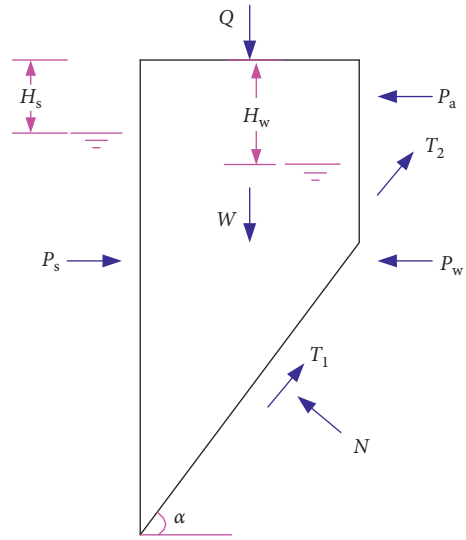

Figure 11: Force analysis of slide mass.

where h_i and h_j are the thickness of soil strip; take h_i, $h_j = a/n$; θ_i can be obtained according to the corresponding geometric relations; and T_i and T_j can be obtained from the static equilibrium on the microstrip, as shown in the following equation:

$$\begin{cases} T_i = \{c\sin\theta_i + [\gamma_s(H - H_s - a\cos\theta_i) - \gamma_w(H - H_w - a\cos\theta_i)]\tan\varphi\} \cdot \dfrac{h_i}{\sin\theta_i + \cos\theta_i\tan\varphi}, \\ T_j = \{c\cos\theta_j + [\gamma_s(H - H_s - a\sin\theta_j) - \gamma_w(H - H_w + a\sin\theta_j)]\tan\varphi\} \cdot \dfrac{h_j}{\cos\theta_j - \sin\theta_j\tan\varphi}. \end{cases} \tag{12}$$

5.3. Design Method and Application Verification of Slurry Unit Weight for Groove Construction Based on Wall Stability. Equations (8) and (10) are the calculation formulas of critical slurry unit weight considering overall stability and local stability of trench wall, respectively, for a specific project; the rest of the parameters of both equations are considered to be certain; therefore, the critical slurry unit weight γ_s can be obtained by selecting the appropriate safety factor. Meanwhile, from the perspective of safety, the larger value of both is selected as the designed value of slurry unit weight in the practical application, that is,

$$\gamma_{s\min} = \max\{\gamma_{sz}, \gamma_{sj}\}, \tag{13}$$

where γ_{sz} is the slurry unit weight calculated by the overall instability model, γ_{sj} is the calculated slurry unit weight by the local instability model, and $\gamma_{s\min}$ is the minimum designed slurry unit weight.

In order to verify the reliability of the above methods, the foundation pit project of Huangxing square station of Changsha metro line 1 in China is taken as the background for specific calculation and application. The project is located in the sand and pebble stratum with rich water; the water table is high, and the formation is permeable; the trench wall is prone to construction risks such as water permeability and even collapse, during the construction process. What is more important, there are many shops around, and the closest distance between the underground diaphragm wall and the shop foundation is only 1.8 m, which may cause serious engineering accidents if it is slightly careless. Therefore, determining reasonable slurry unit weight is the key to ensure the safe and smooth construction of the project.

With reference to geological survey report and design document, the relevant parameters are as follows: groundwater surface H_w is 5 m away from the ground surface, unit weight of groundwater γ_w is 9.8 kN/m^3, trench excavation length L is 6 m, average unit weight of soil mass is 18.8 kN/m^3, ground uniform equivalent load q is 75 kPa, and cohesion force and internal friction angle are 3 kPa and 38°. In the process of trenching construction, the slurry level is located at the surface, that is, $H_s = 0$.

Then, the slurry unit weight γ_{sz} that can ensure the stability of trench wall during the construction of underground diaphragm wall is (10.40, 10.99) kN/m^3 and (12.07, 12.52) kN/m^3, with taking the safety factor as 1.2~1.5. Therefore, according to equation (13), the design value of the slurry unit weight in the groove construction of underground diaphragm wall of this project can be determined as (12.07, 12.52) kN/m^3.

Figures 14 and 15, respectively, show the slurry unit weight and groove quality test results of 5 randomly selected

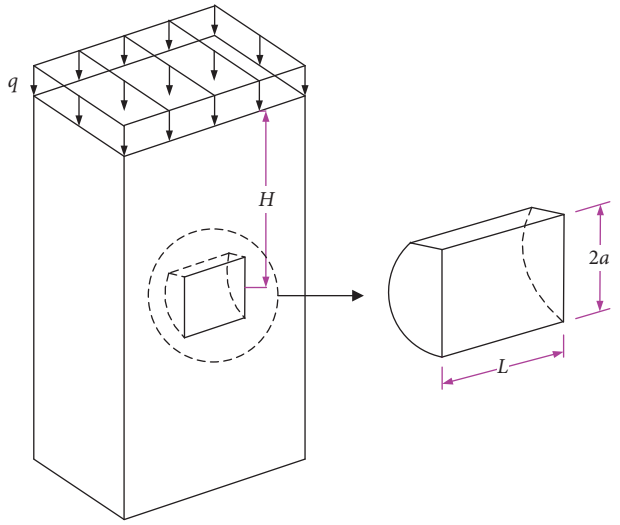

Figure 12: Local sliding model of slot wall. L is the length of the sliding body along the groove section, H is the depth of the sliding body (the distance from the center point of the semicircle column to the surface), and q is the ground overload.

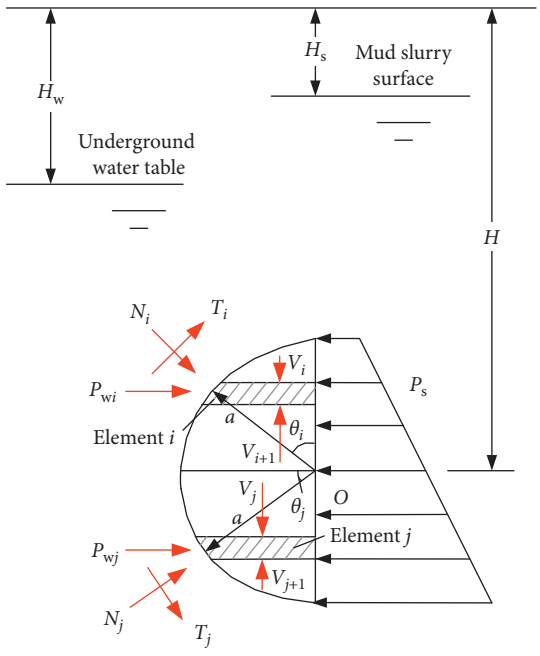

Figure 13: Force analysis of local slide mass.

groove sections in the actual construction process. And from that analysis, the following are observed:

(1) There is a certain degree of inclination in the groove section, but the measured slurry unit weight in each groove section is greater than the designed slurry value of the overall stability of the trench wall, and the trench wall is in a stable state on the whole without overall instability, which is consistent with the theoretical results.

(2) The slot B32 B26 slurry unit weight is relatively smaller, both of them are smaller than the design parameters of locally stable wall protection slurry, and the test result displays that several local spalling and instability phenomena occurred in both sections, and the overall quality of the groove wall was not as good as that of the other three sections. These results show that when the slurry reaches the minimum value obtained by the local stability theory, the trench wall is basically stable during the construction of the underground diaphragm wall.

Based on the above analysis results, it can be seen that the above method is reliable.

6. Stability Factors of Slurry Wall Trench and Its Influencing Laws

6.1. Groundwater Level. The influence of the groundwater level is mainly reflected in the difference between the pressures inside and outside the slurry wall trench. On the one hand, the slurry pressure must be larger than the groundwater pressure for balancing partial earth pressure; therefore, wall protection of hydrostatic pressure of slurry can play [50]. On the other hand, such pressure difference leads to the formation of mud cake and slurry particles on the wall surface. If the pressure difference is small, then a mud cake cannot be easily formed and the slurry particles cannot enter the soil. Therefore, the gelling action of the slurry cannot be played. The groundwater level directly affects the stability of the slurry wall trench. Many experimental studies and engineering practices [9, 10, 12, 13, 16–18, 25, 26, 31, 51] have verified the above views and clearly pointed out that the relative difference between the slurry and groundwater levels is a control condition for the stability of the slurry wall trench. In actual construction practice, the slurry level must be set 1 m to 1.5 m higher than the groundwater level [50, 52].

6.2. Length of the Unit Groove Segment. The length of the unit groove segment can determine the length depth ratio of the groove hole, which in turn influences the soil arc effect and earth pressure. Generally, a large length depth ratio corresponds to a small soil arc effect and a highly unstable slurry wall trench, as shown in Figure 16 [53]. The author investigated the soil arc effect (spatial effect) of the pit wall as an excavating foundation pit and found that the construction has a significant spatial effect for the narrow groove hole similar to the foundation pit. When the unit excavated segment is longer, the space effect is only observed within a certain range of the end part, and the middle part can be regarded as a plane problem. A shorter unit excavated segment has a more significant spatial effect and shows a declining trend in a paracurve from the end part. In actual construction projects, the length depth ratio of an excellent segment ranges between 0.3 and 0.5 (if the excavated depth is larger, then the minimum value is taken; otherwise, the maximum value is taken) [54]. Therefore, for the common foundation pit of a subway station, the excavated depth is about 20 m. Around 5 m to 6 m of the unit segment must be taken, and the soil arc effect must be played.

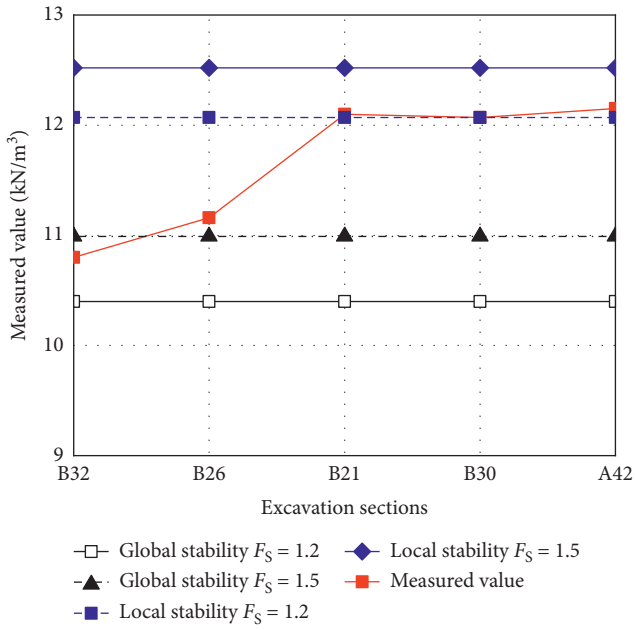

FIGURE 14: Comparison between measured and calculated results of slurry unit weight.

6.3. Slurry Quality. Based on the above discussion, the slurry must have a certain density and consistency to achieve wall protection. Many studies and practices have proven that with a larger density, the slurry can produce a highly significant hydrostatic pressure and the slurry wall trench becomes highly stable (Figure 17) [53]. In practice, the density of the slurry must exceed 10.3 kN/m^3. A slurry with a large density also has a large shear strength, thereby increasing its gelling action and improving the stability of the groove hole [55]. The most commonly used bentonite slurry is formed by mixing 4% to 8% of the total mass of bentonite with water. The resulting slurry has a viscosity of approximately 3×10^{-5} kPa·s and shear strength of less than 7×10^{-3} kPa.

6.4. Soil Conditions of the Foundation. Geographic condition is amongst the key factors that affect the stability of the groove hole. Apart from its shear strength (as shown in the experiment [53], if the cohesion and internal friction angle of the soil are small, then the slurry wall trench can easily collapse), soil density, grain-size composition, and particle size also affect the stability of the groove hole.

If the soil has a high density and excellent grain-size composition, then the slurry cannot be easily lost, and a dense mud cake can be easily formed on the slurry wall trench to protect its stability. By contrast, a mud cake cannot be easily formed if the soil has low density and poor grain-size composition and if the slurry wall trench has increased water permeability. The long seepage path can also result in the loss of slurry and reduce the stability of the slurry wall trench. Given the difference between the water pressure on the both sides of the slurry wall trench and slurry pressure ΔP, the critical hydraulic gradient i_{cr} can be calculated according to equation (14). The maximum distance of the slurry permeating into the surface soil of the slurry wall trench is denoted by l [56], and the retention critical hydraulic gradient can be used to analyse the local stability of the slurry wall trench:

$$i_{cr} = \frac{\Delta P}{\gamma_w l} = \frac{9.3\tau_m}{\gamma_w d_5 e}, \tag{14}$$

where γ_w is the unit weight of water, τ_m is the shear yield stress that the slurry must overcome, e is the void ratio of soil, and d_5 is the size of the soil particles with content of less than 5% of their size.

In groove excavation, the soil particles of the original formation will enter the slurry, and some small particles are suspended in the slurry to increase its density and improve the stability of the slurry wall trench. The maximum size of soil particles suspended in the slurry can be calculated using equation (15) [13]. Li and Deng [57] analyzed the force of the rigid body of a single soil particle and the contact relationship amongst soil particles (Figure 18) and obtained the similar results as shown in equation (16):

$$d = \frac{6\tau_s}{\gamma' - \gamma_s}, \tag{15}$$

$$\begin{cases} d = \dfrac{3\pi}{2}\dfrac{\tau_s}{\gamma' - \gamma_s}, & \text{considering the contact relation between the soil particles,} \\ d = \dfrac{3\pi}{2\sin\phi}\dfrac{\tau_s}{\gamma' - \gamma_s}, \quad \phi = \alpha - \beta, & \text{considering the individual soil particle only,} \end{cases} \tag{16}$$

where γ' is the unit weight of soil particle, β is the angle between the wall surface and the vertical line, and α is the angle between the tangent line at the contact point of two spherical particles and the vertical line.

When the slurry-supported excavation is performed during the formation with a large gravel soil particle, the unit weight of the slurry does not greatly increase because of the suspension of soil particles, thereby contributing minimally to slurry wall trench stability improvement. The ratio of the fresh slurry must be increased to improve the unit weight of the slurry and meet the wall protection pressure that is required for stability.

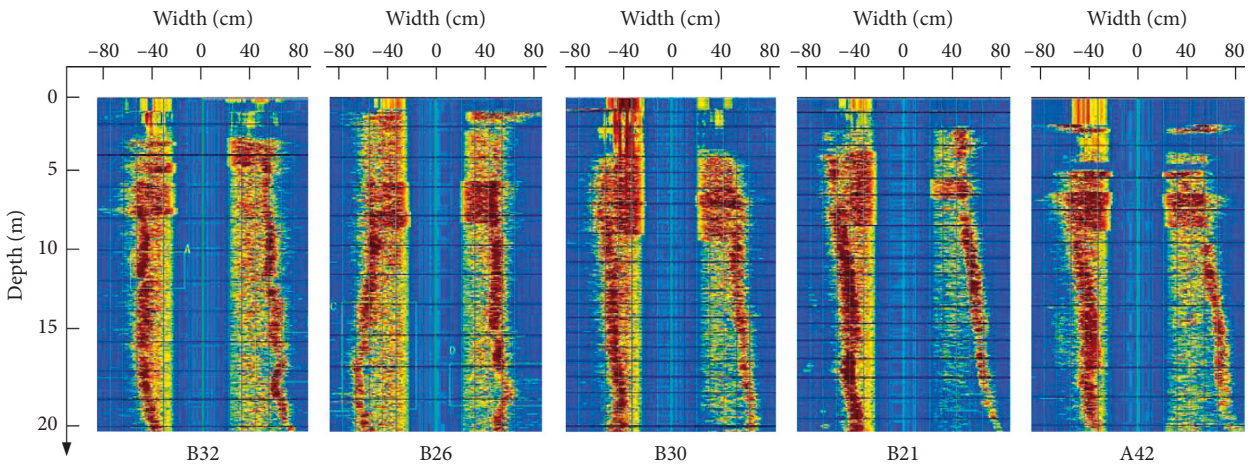

Figure 15: Detection results of trenching quality by ultrasonic testing.

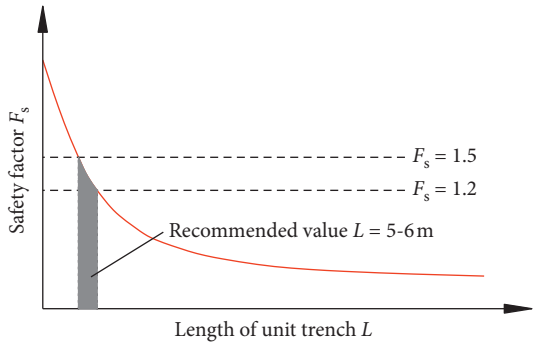

Figure 16: Relationship between trench length and safety factor [53].

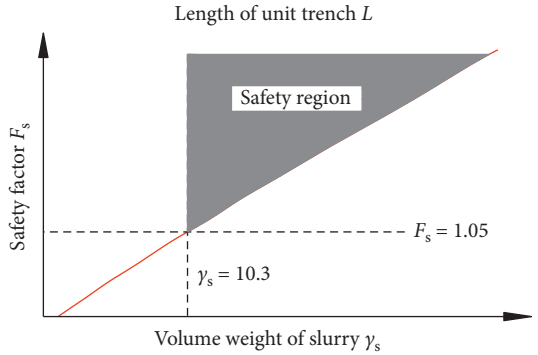

Figure 17: Relationship between slurry gravity and safety factor [53].

6.5. Excavating Machine. The excavating machine can also affect the stability of the slurry wall trench. The weight and oscillation of the machine (equivalent to overload) does not benefit the stability of the slurry wall trench [50], and the up and down movement of the mechanical digging bucket during the excavation will cause the slurry to flow inside the hole. On the one hand, such movements will increase the hole water pressure near the slurry wall trench [58]. On the other hand, a high-speed up and down movement will encourage

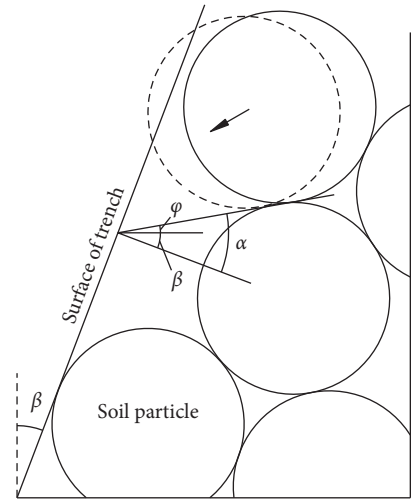

Figure 18: Sketch diagram of soil particle stability analysis [57].

the turbulent flow of the slurry and lead to the erosion of mud cake on the surface of the slurry wall trench and soil particles, thereby resulting in the local destruction and overall instability of the slurry wall trench. Therefore, in actual construction projects, a guide wall with a height of 1 m to 2 m must be added to improve the stability of the surface soil, whilst the up and down movement speed of the mechanical digging bucket must be restricted to reduce the risk of slurry wall trench instability resulting from mechanical excavation.

However, how can a reasonable speed of such up and down movement be determined? In 1985, J. Washbourne performed a relative study by taking the circular shaft as an example (Figure 19) and found that the flow state of the slurry (laminar or turbulent flow) could be used to determine a reasonable movement speed for the mechanical digging bucket. The flow state of the slurry can be determined by the friction coefficient of Bingham fluid and the relationship between the Hearst Roma and Reynolds numbers, as shown in equation (17). To achieve a laminar flow, the movement speed must be kept as low as possible and should not exceed 1 m/s [59]:

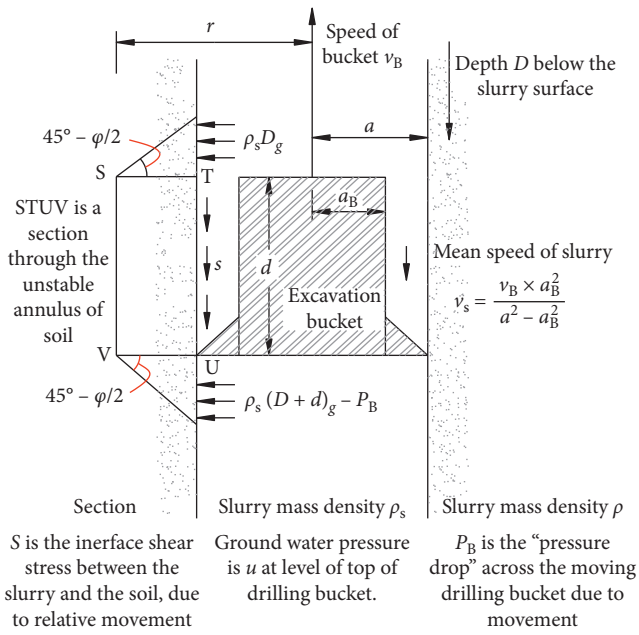

Figure 19: Analysis diagram of slurry flow induced by raise and fall of bucket [59].

$$\begin{cases} v_s = \dfrac{A_k v_w}{A_k - A_w}, \\ D = \dfrac{4(A_k - A_w)}{p_{kw}}, \\ H_e = \dfrac{\tau_s D^2 \rho_s}{\mu_s^2}, \\ R_e = \dfrac{v_s D \rho_s}{\mu_s}, \end{cases} \tag{17}$$

where v_w and v_s are the lifting speed of bucket and flow speed of the slurry, A_k and A_w are the area of the excavated groove mouth and the sectional area of the bucket, D is the equivalent hydraulic diameter of the slurry flow, and $(A_k - A_w)$ is the sectional area of the slurry flow. Moreover, p_{kw} is the wetted perimeter of the slurry flow or the perimeter of the boundary amongst the slurry, wall, and bucket; H_e and R_e are the Hearst Roma and Reynolds numbers; and τ_s, ρ_s, and μ_s are the shear strength, density, and cohesion of the slurry.

6.6. Trench Excavation Sequence. The trench excavation sequence has a certain influence on the stability of the slurry wall trench. Apart from improving the stability of the excavation, the interval construction is more conducive to the soil arc effect of the foundation than the sequential construction [50]. If the excavation period or standing time of the trench is too long, then the slurry will flocculate and deposit. The unit weight of the slurry will be reduced, and its hydrostatic pressure will be weakened. At the same time, the negative hole water pressure caused by the excavation will dissipate. In sandy formation, the stability of the slurry wall trench will decrease [29]. Therefore, a steel reinforcement cage must be placed and concrete or any impervious material must be poured timely after the excavation.

7. Conclusions

This paper performs an extensive literature review and investigates the stability of the slurry wall trench of diaphragm wall panel trenches. The following conclusions are obtained:

(1) The failure mode of the slurry wall trench instability can be divided into two types, namely, overall instability and local stability. The overall instability often occurs about 5 m to 15 m deep into the surface soil, whilst the local instability often occurs in the weak interlayer with a poor bonding property. Therefore, we must explore the formation structure in depth in actual construction projects. Grouting reinforcement is also necessary for the surface soil or weak interlayer to increase the stability of the slurry wall trench.

(2) Given the soil arc effect (spatial effect), the theoretical analysis model or method for the stability of the slurry wall trench can be divided into 2D and 3D types. Scholars all over the world have raised or established more than 10 models or methods for such stability. However, these models or methods have generated varying results because of their different mechanical principles and influencing factors. Comparatively, the calculation results of the 3D model are more reliable and stable than that of the 2D model. Therefore, more research focuses on how to establish an accurate and effective theoretical analysis model should be developed in future.

(3) A consensus regarding the mechanism of the slurry-supported protection has been reached. Researchers universally believe that such mechanism has a hydrostatic pressure action and gelling effect, both of which are related to the quality of the mud cake formation. However, up to now, no theoretical results have been presented from calculating the mud cake thickness and its mechanical or mathematical relationship with slurry quality (including density) for reference. This problem must be addressed to understand further the mechanism of the slurry-supported protection. Therefore, this problem presents both a focus and a challenge to future research.

(4) Many factors affect the stability of the slurry wall trench, and each factor has a different function mechanism and influencing law. Generally, the excavated length for the unit segment and slurry level are critical parameters that influence the stability of the slurry wall trench. In actual construction projects, the excavated length of the unit segment must be controlled within 5 m to 6 m, and the slurry level must be always set between 1 m and 1.5 m higher than the groundwater level.

Also, based on the limit equilibrium theory, mechanical analysis models of overall and local stability of trench wall during the process of grooving construction of underground diaphragm wall are established, and the formulas for calculating the slurry unit weight of trench wall are derived. The example shows that the calculation method of slurry unit weight is reliable.

Nomenclature

F_s, $[F_s]$: Computational and design safety factor of slurry wall trench
r_1, r_2, and r_3: Radius of Mohr's circle of element soil before, behind the excavation, and its limit state
p_s and P_s: Slurry pressure in trench and its resultant force
p_w and P_w: Water pressure and its resultant force
p and P: Lateral earth pressure and its resultant force
σ_1 and σ_3: Vertical and horizontal stress of slurry wall trench soil
L, $w = 2b$, and d: Length, width, and depth of groove
γ, γ', ϕ, c, and e: Unit weight, dry unit weight, internal friction angle, cohesion, and void ratio of soil
K, K_a, and K_0: Earth pressure coefficient considering the soil arc effect, active earth pressure coefficient, and static earth pressure coefficient
τ_f: Shear strength of soil
τ_s, ρ_s, and μ_s: Shear strength, density, and viscosity of slurry
Δp: The difference between the water pressure on the both sides of the slurry wall trench and slurry pressure
i_{cr}: The critical hydraulic gradient
l: The maximum distance of the slurry permeating into the surface soil of the slurry wall trench
γ_w: Unit weight of water
d_5: The size of the soil particles with a content less than 5% of their size
α and β: The angle between the tangent line at the contact point of two spherical particles and the vertical line and the angle between the wall surface and the vertical line
v_w and v_s: The lifting speed of bucket and flow speed of the slurry
A_k, A_w, and $(A_k - A_w)$: The area of the excavated groove mouth and the sectional area of the bucket and the sectional area of the slurry flow
D: The equivalent hydraulic diameter of the slurry flow
p_{kw}: The wetted perimeter of the slurry flow or the perimeter of the boundary amongst the slurry, wall, and bucket
H_e and R_e: Hearst Roma and Reynolds numbers
h_w and h_s: Slurry level and underground water level
q: Overload around the groove
Z and z: Depth direction of groove and the depth of calculating point.

Conflicts of Interest

The authors declare that they have no conflicts of interest.

Acknowledgments

Projects funded by the National Natural Science Foundation of China (no. 51978669 and U1734208), the Natural Science Foundation of Hunan Province, China (no. 2018JJ3657), and the Fundamental Research Funds for the Central Universities of Central South University (no. 2019zzts294) are gratefully acknowledged.

References

[1] Y.-C. Li, Q. Pan, P. J. Cleall, Y.-M. Chen, and H. Ke, "Stability analysis of slurry trenches in similar layered soils," *Journal of Geotechnical and Geoenvironmental Engineering*, vol. 139, no. 12, pp. 2104–2109, 2013.

[2] K. L. Nash, "Stability of trenches filled with fluids," *Journal of the Construction Division*, vol. 100, no. 4, pp. 533–542, 1974.

[3] S. Zhang, J. Li, Q. Liu et al., "Application of underground diaphragm wall in subway projects," *Journal of Tianjin Municipal Engineering*, vol. 20, no. 3, pp. 25–27, 2008, in Chinese.

[4] M. Lei, D. Lin, Q. Huang, C. Shi, and L. Huang, "Research on the construction risk control technology of shield tunnel underneath an operational railway in sand pebble formation: a case study," *European Journal of Environmental and Civil Engineering*, vol. 22, pp. 1–15, 2018.

[5] M. Lei, D. Lin, C. Shi, J. Ma, and W. Yang, "A structural calculation model of shield tunnel segment: heterogeneous equivalent beam model," *Advances in Civil Engineering*, vol. 2018, Article ID 9637838, 16 pages, 2018.

[6] China Association of Metros (CAM), "2015 Annual report of China urban mass transit," Report, China Association of Metros, Beijing, China, 2016.

[7] M. Lei, D. Lin, J. LIU et al., "Modified chloride diffusion model fir concrete under the coupling effect of mechanical load and chloride salt environment," *AIP Advances*, vol. 8, no. 3, Article ID 035029, 2018.

[8] J. Zhang and L. Han, "Method and effect for controlling slum ping trench section of continuous concrete wall in Huangsha Station along Guangzhou subway," *Foundation Engineering*, vol. 9, no. 4, pp. 52–55, 1999, in Chinese.

[9] J. Dai, "Collapse analysis of underground diaphragm wall," *China Water Transport*, vol. 14, no. 6, pp. 372-373, 2014, in Chinese.

[10] G. C. Y. Wong, "Stability analysis of slurry trenches," *Journal of Geotechnical Engineering*, vol. 110, no. 11, pp. 1577–1590, 1984.

[11] W. Shengwei, "Study on construction technology of trough-forming of diaphragm wall in super-deep foundation pit under complex geological condition," *Railway Engineering*, vol. 50, no. 12, pp. 51–54, 2010, in Chinese.

[12] J.-S. Tsai, L.-D. Jou, and H.-S. Hsieh, "A full-scale stability experiment on a diaphragm wall trench," *Canadian Geotechnical Journal*, vol. 37, no. 2, pp. 379–392, 2000.

[13] N. Mogrenstern and I. Amir-Tahmasseb, "The stability of a slurry trench in cohesionless soils," *Géotechnique*, vol. 15, no. 4, pp. 387–395, 1965.

[14] T. Tamano, H. Q. Nguyen, M. Kanaoka et al., "Deformation and failure of slurry trench in reclaimed soft clay: numerical analysis," in *Proceedings of the 12th Asian Regional Conference on Soil Mechanics and Geotechnical Engineering*, vol. 1, pp. 825–828, World Scientific Publishing, Singapore, August 2003.

[15] J.-S. Tsai, C.-C. Chang, and L.-D. Jou, "Lateral extrusion analysis of sandwiched weak soil in slurry trench," *Journal of Geotechnical and Geoenvironmental Engineering*, vol. 124, no. 11, pp. 1082–1090, 1998.

[16] G. Li, "Cause analysis of ground collapsing in the construction of cutoff wall in the saddle dam of Huangbizhuang reservoir," *Technical Supervision in Water Resources*, vol. 11, no. 2, pp. 43–47, 2003, in Chinese.

[17] H. Li and S. Wang, "Experimental and limit equilibrium research on the stability of underground diaphragm wall," *Shanxi Construction*, vol. 18, no. 3, pp. 27–31, 1992, in Chinese.

[18] G. Aas, "Stability of slurry trench excavations in soft clay," in *Proceedings of the 6th European Conference on Soil Mechanics and Foundation Engineering*, pp. 103–110, International Society of Soil Mechanics and Foundation Engineering, Vienna, Austria, March 1976.

[19] J. Washbourne, "The three-dimensional stability analysis of diaphragm wall excavations," *Ground Engineering*, vol. 17, no. 4, pp. 24–29, 1984.

[20] C. Valore, M. Ziccarelli, and S. R. Muscolino, "The bearing capacity of footings on sand with a weak layer," *Geotechnical Research*, vol. 4, no. 1, pp. 12–29, 2017.

[21] C. Y. Han, J. H. Wang, X. H. Xia et al., "Limit analysis for local and overall stability of a slurry trench in cohesive soil," *International Journal of Geomechanics*, vol. 15, no. 5, Article ID 06014026, 2012.

[22] D. Gong, *Research on the Foundation Pit Construction Technology of Changsha Metro Station in the Water-Rich Sandy Cobble Strata of Densely Built-Up Areas*, Central South University, Changsha, China, 2013, in Chinese.

[23] J.-S. Tsai, "Stability of weak sublayers in a slurry supported trench," *Canadian Geotechnical Journal*, vol. 34, no. 2, pp. 189–196, 1997.

[24] J. K. T. L. Nash and G. K. Jones, "The support of trenches using fluid mud," in *Proceedings of Grouts and Drilling Muds in Engineering Practice*, pp. 177–180, Butterworths, London, UK, May 1963.

[25] W. K. Elson, "An experimental investigation of the stability of slurry trenches," *Géotechnique*, vol. 18, no. 1, pp. 37–49, 1968.

[26] P. Oblozinsky, K. Ugai, M. Katagiri et al., "A design method for slurry trench wall stability in sandy ground based on the elasto-plastic FEM," *Computers and Geotechnics*, vol. 28, no. 2, pp. 145–159, 2001.

[27] C. E. Grandas-Tavera and T. Triantafyllidis, "Simulation of a corner slurry trench failure in clay," *Computers and Geotechnics*, vol. 45, pp. 107–117, 2012.

[28] A. J. Li, R. S. Merifield, H. D. Lin, and A. V. Lyamin, "Trench stability under bentonite pressure in purely cohesive clay," *International Journal of Geomechanics*, vol. 14, no. 1, pp. 151–157, 2014.

[29] P. Jiang, Z. Hu, and J. Liu, "Analysis of space-time effect on the stability for slurry-trench of diaphragm wall," *Chinese Journal of Geotechnical Engineering*, vol. 21, no. 3, pp. 338–342, 1999, in Chinese.

[30] G. Liu, Y. Huang, and J. Liu, "Analysis of the stability of slurry trench with a surchargeand engineering application," *Journal of Tongji University*, vol. 28, no. 3, pp. 267–271, 2000, in Chinese.

[31] I. Hajnal, J. Marton, and Z. Regele, *Construction of Diaphragm Walls*, John Wiley & Sons, New York, NY, USA, 1984.

[32] J. Huder, "Stability of bentonite slurry trenches with some experiences in Swiss practice," in *Proceedings of the 5th European Conference on Soil Mechanics and Foundation Engineering*, vol. 4, no. 9, pp. 517–522, Madrid, Spain, April 1972.

[33] R. Yang, "The clear solution of the critical specific gravity of slurry propping the trench of diaphragm wall- the bottom of slump mass does not cross the groundwater level," *Journal of Nanjing Architectural and Civil Engineering Institute*, vol. 32, no. 1, pp. 22–28, 1995, in Chinese.

[34] R. Yang, "Iteration methods calculating the critical specific gravity of slurry propping the trench of diaphragm wall-in case that the bottom of slump mass crosses ground water surface and does not ground surface," *Journal of Nanjing Architectural and Civil Engineering Institute*, vol. 34, no. 3, pp. 42–49, 1995, in Chinese.

[35] R. Yang and S. Liu, "Stability analysis of slurry trench side of diaphragm wall near ground surface-slurry critical specific gravity in case that the bottom of slump mass crosses ground surface," *Journal of Nanjing Architectural and Civil Engineering Institute*, vol. 41, no. 2, pp. 28–34, 1997, (in Chinese).

[36] L. Li, "Formula discrimination of 3-D analysis of trenches stability," *Chinese Journal of Geotechnical Engineering*, vol. 23, no. 3, pp. 374-375, 2001, in Chinese.

[37] C. Ji and S. Yu, "The stability of slurry trench diaphragm wall," *Journal of East China Jiaotong University*, vol. 15, no. 3, pp. 13–17, 1998, (in Chinese).

[38] A. Piaskowski and Z. Kowalewski, "Application of thixotropic clay suspensions for stability of vertical sides of deep trenches without strutting," in *Proceedings of the 6th International Conference on Soil Mechanics and Foundation Engineering*, vol. 2, pp. 526–529, Montreal, Canada, September 1965.

[39] H. Zhang and M. Xia, "3-D stability analysis of slurry trenches," *China Civil Engineering Journal*, vol. 33, no. 1, pp. 73–76, 2000, in Chinese.

[40] J.-S. Tsai and J.-C. Chang, "Three-dimensional stability analysis for slurry-filled trench wall in cohesionless soil," *Canadian Geotechnical Journal*, vol. 33, no. 5, pp. 798–808, 1996.

[41] G. M. Filz, T. Adams, and R. R. Davidson, "Stability of long trenches in sand supported by bentonite-water slurry," *Journal of Geotechnical and Geoenvironmental Engineering*, vol. 130, no. 9, pp. 915–921, 2004.

[42] C.-y. Han, J.-j. Chen, J.-h. Wang, and X.-h. Xia, "2D and 3D stability analysis of slurry trench in frictional/cohesive soil," *Journal of Zhejiang University Science A*, vol. 14, no. 2, pp. 94–100, 2013.

[43] P. J. Fox, "Analytical solutions for stability of slurry trench," *Journal of Geotechnical and Geoenvironmental Engineering*, vol. 130, no. 7, pp. 749–758, 2004.

[44] X. Wang, G. Lei, and J. Shi, "Comparative study of global stability analysis methods of rectangular diaphragm wall panel trenches," *Rock and Soil Mechanics*, vol. 27, no. 4, pp. 549–554, 2006, in Chinese.

[45] Q. Huai and X. Song, "A brief analysis of slurry mechanism and its application," *West-China Exploration Engineering*, vol. 20, no. 7, pp. 81–83, 2008.

[46] H.-c. Zhuo, Y.-y. Yang, Z.-x. Zhang, C.-h. Pan, and C.-f. Duan, "Stability of long trench in soft soils by bentonite-

water slurry," *Journal of Central South University*, vol. 21, no. 9, pp. 3674–3681, 2014.

[47] P. P. Xantakos, *Slurry Walls as Structural Systems*, McGraw-Hill, New York, NY, USA, 2nd edition, 1994.

[48] L. Russo and R. S. Wanapum, "Development-slurry trench and grouted cut-off," in *Proceedings of Symposium: Grouts and Drilling Mudsin Engineering Practice*, pp. 95–102, Buttreworths, London, UK, May 1963.

[49] S. A. Gill, "Applications of slurry walls in civilengi-neering," *Journal of Construction Division*, vol. 106, pp. 156–167, 1980.

[50] G. Lei, X. Wang, and G. Lei, "Stability influencing factors and instability mechanism of slurry—supported excavations," *Advances in Science and Technology of Water Resources*, vol. 26, no. 1, pp. 82–86, 2006, in Chinese.

[51] T. Tamano, S. Fukui, H. Suzuki, and K. Ueshita, "Stability of slurry trench excavation in soft clay," *Soils and Foundations*, vol. 36, no. 2, pp. 101–110, 1996.

[52] A. Ueshita, "Effect of groundwater table rising and slurry reduction during diaphragm wall trenching on stability of adjacent piles," in *Proceedings of the 2015 International Symposium on Geohazards and Geomechanics (ISGG2015)*, pp. 50–54, Warwick, UK, September 2015.

[53] S. Shi and W. Zhang, "Stability analysis of slurry trench of diaphragm in deep excavation," *Chinese Journal of Geotechnical Engineering*, vol. 28, no. suppl, pp. 1418–1421, 2006, in Chinese.

[54] M. F. Lei, L. M. Peng, C. H. Shi, Y. L. Zhang, and W. H. Zhang, "A simplified calculation method for spatial effect in large-long-deep foundation pit and its analysis," *Advanced Materials Research*, vol. 243–249, pp. 2762–2770, 2011.

[55] Z. Wang, "Hole wall instability and mechanism of slurry protection about large diameter bilge well," *Journal of Central South University (Science and Technology)*, vol. 43, no. 12, pp. 4859–4864, 2012, in Chinese.

[56] G. M. Filz, R. D. Boyer, and R. R. Davidson, "Bentonite-water slurry rheology and cutoff wall trench stability," in *Proceedings of the Situ Remediation of the Geoenvironment*, no. 71, pp. 139–153, ASCE, Minneapolis, MN, USA, October 1997.

[57] S. Li and W. Deng, "The study of the mechanism of dado with slurry," *Journal of Fuxin Mining Institute*, vol. 9, no. 2, pp. 11–15, 1990, in Chinese.

[58] T. Hosoi, A. S. Balasubramanisa and D. T. Bergado, Increase in pore water pressure during excavation," in *Proceedings of Geotech-Year 2000, Developments in Geotechnical Engineering*, vol. 1, pp. 243–252, Bangkok, Thailand, 2000.

[59] J. Washbourne, "The stability of vertical shaft excavations," *Ground Engineering*, vol. 18, pp. 16–19, 1985.